



# A photonic artificial synapse with a reversible multifaceted photochromic compound†

Cite this: DOI: 10.1039/d2nh00532h

Deeksha Sharma, <sup>ab</sup> Dheemahi Rao <sup>ab</sup> and Bivas Saha <sup>\*abc</sup>Received 10th November 2022,  
Accepted 14th February 2023

DOI: 10.1039/d2nh00532h

rsc.li/nanoscale-horizons

Modern computational technology based on the von Neumann architecture physically partitions memory and the central processing unit, resulting in fundamental speed limitations and high energy consumption. On the other hand, the human brain is an extraordinary multifunctional organ composed of more than a billion neurons capable of simultaneously thinking, processing, and storing information. Neurons are interconnected with synapses that control information flow from pre-synaptic-to-post-synaptic neurons. Therefore, emulating synaptic functionalities and developing neuromorphic computational architecture has recently attracted much interest. Due to their high-speed, large bandwidth, and no interconnect-related power loss, photonic (all-optical) synapses can overcome the existing hurdles with electronic synapses. Here, we show an artificial photonic synapse by utilizing the well-established reversible, high-contrast photochromic organic compound, spiropyran, stimulated by optical pulses. Optical transmission of spiropyran significantly changes during spiropyran–merocyanine isomerization driven by UV-visible optical pulses. Such changes are equivalent to the biological synapses' inhibitory and excitatory synaptic actions. The slow relaxation to the initial state is considered as synaptic plasticity responsible for learning and memory formation. Short-term memory (STM), long-term memory (LTM), and transition from the STM to the LTM are demonstrated in all-optical synapses by modulating the stimuli's strength. The solvatochromic properties of spiropyran are further utilized to augment memory in synapses. Our work shows that photochromic organic compounds are excellent hosts for artificial photonic synapses and can be implemented in neuromorphic applications.

In the modern scientific era, almost all computing systems work with one fundamental input–output mechanism based on the von Neumann architecture.<sup>1</sup> However, as the future moves towards

## New concepts

All optical synapses with photochromic organic compounds. Traditional computation based on von Neumann architecture is limited by time and energy consumption due to data transfer between the storage and the processing units. The von Neumann architecture is also inefficient in solving unstructured, probabilistic, and real-time problems. To address these challenges, a new brain-inspired neuromorphic computational architecture is required. Due to their high-speed, large bandwidth, and no interconnect-related power loss, photonic (all-optical) synapses can overcome the existing hurdles with electronic synapses. In this work, we show an artificial photonic synapse by utilizing the well-established reversible, high-contrast photochromic organic compound, spiropyran, stimulated by optical pulses. Our work shows that photochromic organic compounds are excellent hosts for artificial photonic synapses and can be implemented in neuromorphic applications.

multiple-institution-multiple-data (MIMD) processing technology for artificial intelligence and machine learning applications, the von-Neumann architecture is increasingly facing severe strain.<sup>2</sup> In the conventional von Neumann system, the memory and central processing units are partitioned and interconnect shuttle information between them. Such physical partitioning limits the rate of information flow between the memory and the processing unit, leading to a longer processing time as each process is performed in a sequence.<sup>3,4</sup> Data transfer through interconnects also consumes a large amount of energy, far exceeding the energy cost per bit operation in the processing unit. Therefore, a new computational architecture that will fundamentally address the existing bottleneck and improve high energy cost and speed issues will significantly enhance the computational capability.

Compared to the present technology, the human brain is one of the most efficient processors that can sense, process,

<sup>a</sup> Chemistry and Physics of Materials Unit, Jawaharlal Nehru Centre for Advanced Scientific Research, Bangalore 560064, India. E-mail: bsaha@jncasr.ac.in, bivas.mat@gmail.com

<sup>b</sup> International Centre for Materials Science, Jawaharlal Nehru Centre for Advanced Scientific Research, Bangalore 560064, India

<sup>c</sup> School of Advanced Materials (SAMat), Jawaharlal Nehru Centre for Advanced Scientific Research, Bangalore 560064, India

† Electronic supplementary information (ESI) available: The impact of UV and visible light pulses on the transmission spectra, NMR spectra, spiropyran-to-merocyanine conversion in the spiropyran polymer composite, transmission spectra of the polymer with demonstrating an inhibitory synapse, and proposed neural network. See DOI: <https://doi.org/10.1039/d2nh00532h>

and store information simultaneously. It is nearly ten times more energy-efficient than a personal computer and exhibits self-learning capability.<sup>5</sup> Such excellent functionalities in the brain arise from more than a billion neurons interconnected with a trillion synapses.<sup>6</sup> Triggered by external stimuli, an action potential (information) travels down an axon of the pre-synaptic neuron to the post-synaptic neuron through the synaptic cleft.<sup>7</sup> This complex physiochemical process polarizes/depolarizes the membrane potential, which will be retained in the synapse as memory. Such in-memory computing ability of the human central nervous system enables it to perform complex operations such as learning, memorizing, thinking, solving probabilistic and stochastic programs, *etc.*, much more efficiently.<sup>8</sup> Therefore, emulating the functionalities of the brain and the development of a neuromorphic system remains one of the most extraordinary challenges in the modern scientific and technological era.

Since synapses are the main building blocks of the nervous system,<sup>9</sup> one of the crucial challenges of brain-inspired computing technology is to emulate synaptic functionalities. Over the last few decades, neuromorphic circuits have been successfully implemented in complementary-metal-oxide-semiconductor (CMOS) chips, such as the TrueNorth chip from IBM,<sup>10</sup> the Loihi chip from Intel,<sup>11</sup> *etc.* However, such systems are incredibly power-hungry<sup>12</sup> and require numerous operations to execute fundamental tasks such as voice and image recognition. With the demonstration of memristors by HP labs in 2008,<sup>13</sup> significant efforts have been made to develop neuromorphic-based hardware systems.<sup>14,15</sup> Artificial synapses<sup>16</sup> made up of phase change materials,<sup>17,18</sup> nanoionics,<sup>19,20</sup> magnetic tunnel junctions<sup>21,22</sup> and transistors<sup>23–25</sup> have been heavily studied over the last five-to-ten years. Basic synaptic functionalities such as short-term memory (STM),<sup>26</sup> long-term memory (LTM),<sup>27</sup> frequency-selective optical filtering, frequency-dependent potentiation and depression, Hebbian learning, and logic-gate operations are well demonstrated. However, most synapse-like hardware is electronic, where external electrical pulses control the current flow. As a result, they suffer from resistance-capacitance (RC) delays, exhibit low bandwidth, and consume high power.<sup>28</sup>

To circumvent these challenges with the electronic synapse, optoelectronic artificial synapses have been developed utilizing photo-responsive materials such as metal oxides,<sup>29</sup> organic materials,<sup>30</sup> perovskites,<sup>31</sup> and 2D materials,<sup>32</sup> including graphene,<sup>33</sup> h-BN,<sup>34</sup> MoS<sub>2</sub>,<sup>35,36</sup> and WSe<sub>2</sub>.<sup>37</sup> In these optoelectronic synapses, current flow between electrodes is controlled by optical stimuli. However, due to their inherent electronic nature, the optoelectronic synapses also suffer drawbacks such as RC delays, low sensitivity, *etc.* The artificial synapse with the filamentary memory phenomenon is one of the electronic synapses where an electric current leads to the formation of a conductive channel providing a path for the migration of ions, also termed a low resistance state. When the voltage polarity changes, the filament breaks, leading to a high resistance memory state responsible for the synaptic behavior.<sup>38</sup> On the other hand, in all-optical artificial synapses, the information flow between two ends of the device and the gate stimuli that

control it are optical and it doesn't involve changes in the resistance for synaptic functionalities. This could provide an ideal solution to the existing challenges of synapse design.<sup>39,40</sup> With photons as both information carriers and stimuli, all-optical synapses exhibit high speed without suffering from RC-delays.<sup>41</sup> In addition, such synapses exhibit a larger bandwidth (frequency range of operation) and no interconnect-related power loss. Photonic synapses based on gallium lanthanum oxysulphide (GLSO) fiber<sup>8,42</sup> and gallium sulfur telluride (GST)<sup>43</sup> phase change material have been shown over the last few years. The data transmission and brain-like activity in the form of plasticity<sup>44</sup> are elucidated in GLSO microfibers using photo-darkening functionality. Similarly, a photonic integrated circuit approach in Ge<sub>2</sub>Sb<sub>2</sub>Te<sub>5</sub> and Si<sub>3</sub>N<sub>4</sub> waveguide is used to obtain the desired synaptic weight. Though these demonstrations of all-optical synapses have heralded a new era of low-power, high-speed photonic neuromorphic systems, they usually require complex lasers and waveguides. At times, they are also wavelength selective, which limits their practical utility. Therefore, photonic synapses that don't need a complex laser system, with minimal fabrication and operation, will significantly benefit this budding research field.

This work elucidates a photonic synapse using a simple photochromic organic chemical, spiropyran. Spiropyran is a family of photochromic organic compounds well-known for its lucid photo-responsivity,<sup>45,46</sup> out of which the 1',3'-dihydro-1'3'3'-trimethyl-6-nitrospiro[2H-1-benzopyran-2,2'-(2H)-indole] derivative has been used in this work. This molecule has chromene and indoline moieties perpendicularly joined at the spiro-junction.<sup>46</sup> The molecule undergoes a photochromic isomerization reaction between the closed-ring spiropyran and open-ring merocyanine forms by breaking the C–O bond distinguished by their characteristic colors.<sup>47</sup> However, the C–O bond in spiropyran is weak, unstable, and highly depends on the environment. In a polar environment like methanol, due to the low solubility of spiropyran, only a few molecules are dissolved and converted to merocyanine, resulting in a light pink solution which is the equilibrium state. When a UV light pulse is irradiated, energy from the 365 nm pulse breaks the rest of spiropyran's C–O bonds, resulting in increased merocyanine isomers and deeper intensity. On visible light (400–800 nm) illumination, the merocyanine isomers convert back to spiropyran, decreasing the color's intensity and increasing transmission. If the light is irradiated for a longer time, then enough merocyanine reverts to spiropyran resulting in a colorless solution. The relaxation to the equilibrium state on removing optical pulses is considered synaptic plasticity and is varied by the optical pulses' strength and the solvent's polarity.

In biological neurons, the electrical signal propagation from a pre-synaptic neuron to a post-synaptic neuron is controlled by the synaptic strength modulated by the stimuli's nature<sup>31</sup> (see Fig. 1(a)). The action potential generated by the external stimuli controls the neurotransmitter release in the synaptic cleft from the pre-synaptic neuron and the transmissibility of the receptors at the post-synaptic neuron. The synapse can either pass on the signal to the next neuron (excitatory) or block the signal

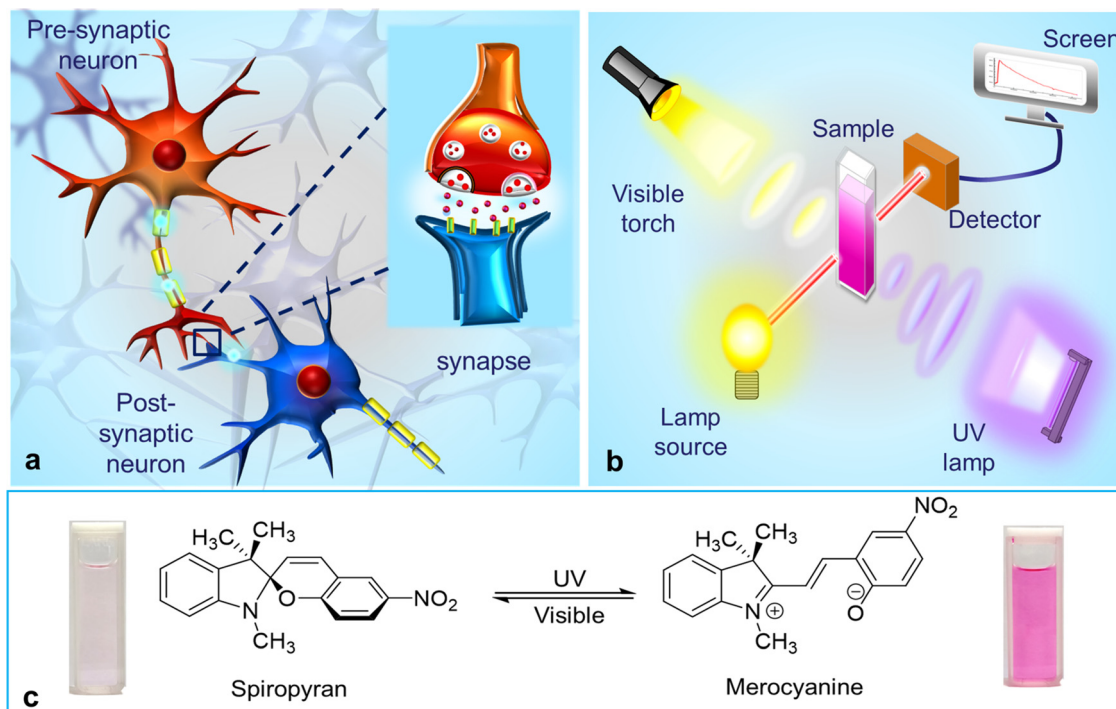


**Fig. 1** (a) Schematic of a biological synaptic junction where the signal is transferred from a pre-synaptic to a post-synaptic neuron. The inset shows a magnified synapse. (b) Schematic of an all-optical artificial synapse mimicking a biological synapse with visible light and a UV lamp of wavelength 365 nm. (c) Reversible photoisomerization of colorless spiropyran and colored merocyanine forms with visible and UV illumination.

(inhibitory) based on its role in the physiological process and simultaneously deform, creating a memory.

An equivalent setup to emulate synaptic activities in an all-optical artificial synapse is shown in Fig. 1(b). Spiropyran solution in methanol is placed in front of a light source serving as a pre-synaptic neuron, while a spectrophotometer collects the transmission spectra resembling a post-synaptic neuron. Variation in synaptic weight is analogous to the changes in the optical transmission through the spiropyran solution caused by visible (400–850 nm) and UV (365 nm) pulses acting as stimuli.

Fig. 1(c) shows the structural and color changes associated with the isomerization by varying light wavelengths.

As discussed, the solution state varies with incident light having an optical transmission spectrum, as shown in Fig. 2(a). The transmission spectrum has a minimum of 527.5 nm ( $\lambda_{\min}$ ). The transmittance at  $\lambda_{\min}$  is the measure of isomer concentration and is taken as a reference for mimicking the synaptic activity. In the dark, the solution has a transmission intensity close to 55% (green curve in Fig. 2(a))<sup>14</sup> because of both spiropyran and merocyanine isomers.<sup>48</sup> Some of the spiropyran

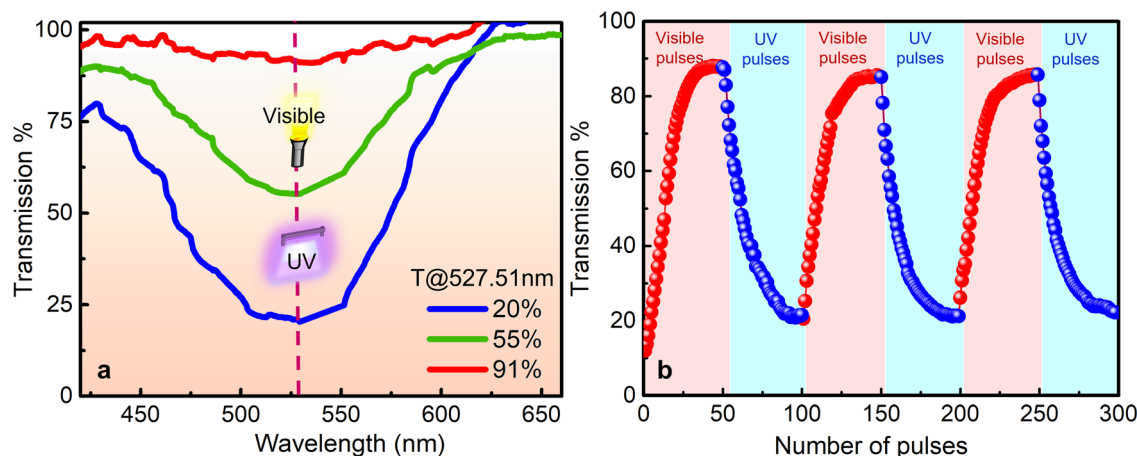


**Fig. 2** (a) Transmission spectra of spiropyran in the dark (intermediate state), under UV illumination (dark pink state), and visible illumination (colorless state). The transmission intensity at 527.5 nm ( $\lambda_{\min}$ ) decreases as the merocyanine concentration increases (solution turns pink). (b) Switching cycle between spiropyran–merocyanine with visible and UV light pulses of 15 s each.

spontaneously forms merocyanine in polar solvents ( $\Delta G < 0$ ),<sup>49</sup> resulting in a pink solution. On UV irradiation, it changes to a dark pink state (more number of merocyanine) with transmittance reduced to 20% (blue transmission curve Fig. 2(a)). The amplified intense color correlates to the spiropyran molecules converting to merocyanine obtaining energy from the UV light. Irradiation with visible light shifts the equilibrium towards a colorless closed spiropyran with an approximate transmission intensity of 91% (red transmission curve 2a). The ring opening and closing with UV and visible light irradiation are validated by the <sup>1</sup>H NMR spectra shown in the ESI.† The switching between the isomers<sup>50</sup> is highly repetitive and reproducible with pulses of corresponding light sources, as shown in Fig. 2(b); with 50 visible pulses of 15 s each, the solution transitions from a colored to a highly transparent one. The UV pulses with the exact count and width bring the system back to the lowest transmission state. The repeatability of this transmission cycle indicates this system's quantum switching ability, stability, and reliability for mimicking neuromorphic functionalities.

Transmission change at  $\lambda_{\min}$  with a single optical pulse relative to the intermediate state (solution in the darkness) is observed for replicating the excitatory and inhibitory synaptic activity. On shining a visible pulse to the intermediate state, the transmittance shifts to a higher value, as shown in Fig. 3(a). As soon as the pulse is removed, this high transmission state gradually undergoes thermal relaxation<sup>46</sup> to its initial state without any stimuli. The system returns to an intermediate state when left in the dark (inset in Fig. 3(a)), with the modified form persisting for almost 3.3 hours. In addition, a UV pulse lowers the transmission intensity, and the occurring change is observed to be retained in the system for more than 4 hours (see Fig. 3(b)). The solution becomes dark pink when irradiated with UV light and relaxes back to the intermediate state shown in the inset image of Fig. 3(b). The increasing and decreasing transmission behavior with a visible pulse and UV pulse are

equivalent to the excitatory and inhibitory synaptic functions, respectively. The time duration for the pulse-driven change to reach the intermediate state is analogous to the synaptic plasticity forming the system's memory. The longer the time taken to get the initial transmission value, the more the plasticity will be, and hence the memory. It is important to note that unlike in the previous demonstration of GLSO photonic synapses, where an optical bias with pre-assigned intensity is applied to introduce the intermediate state, the intermediate state obtained in this work is an intrinsic nature of the system arising from the solute-solvent interactions. Similarly, the memory in the spiropyran-based photonic synapse demonstrated here lasts for several hours compared to the GLSO photonic synapses, where it survives only for a few minutes.

A short-term change produced by a pulse in the synaptic strength leads to short-term memory (STM), where the applied change stays for only a few seconds. Long-term memory (LTM) is achieved when the stimuli are strong enough to retain the difference for up to a few minutes or hours.<sup>51</sup> The STM to LTM transition can be studied by changing the stimuli's exposure duration, number, frequency, or intensity.<sup>52</sup> In this work, the STM-to-LTM conversion is shown by varying the time and number of stimuli pulses. In an excitatory synapse, the percentage transmission changes by altering the pulse duration from 1 minute to 3 minutes, signifying a modified synaptic weight (Fig. 4(a)). Higher transmission intensity indicates a higher spiropyran concentration in the solution. This, in turn, increases the time for the molecules to relax back to their intermediate equilibrium state. Thus, with increased pulse duration, synaptic plasticity also increases. Similar results can also be seen in the case of inhibitory synapses (Fig. 4(c)). In this case, the lowered transmission intensity is due to merocyanine isomers that relax to equilibrium once the radiation is removed. In the case of changing number of pulses, transmission increases (decreases) for the excitatory (inhibitory) optical signal (Fig. 4(b) and (d)), which highlights the transition. Thus,

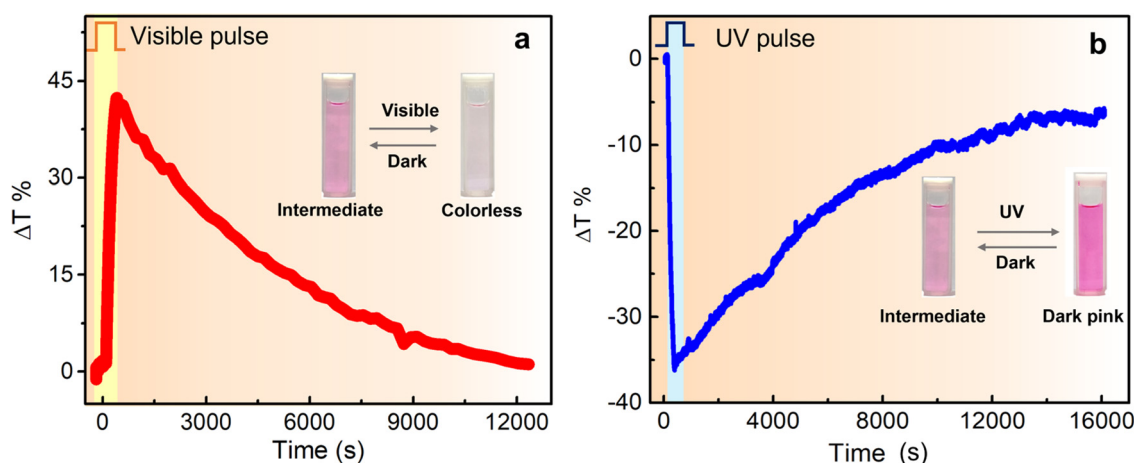
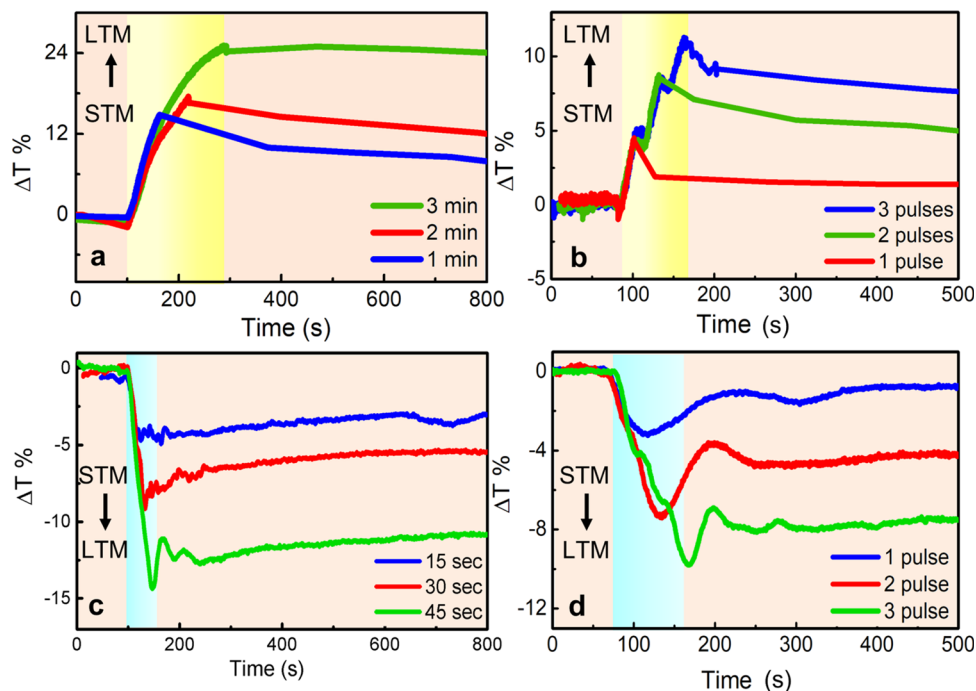


Fig. 3 Emulating (a) an excitatory synapse with a visible pulse and (b) an inhibitory synapse with a UV pulse. The inset shows the visible color changes during the process. The time taken for transmission to return to its initial state is equated to synaptic plasticity that is responsible for memory formation.



**Fig. 4** The transition from STM-to-LTM where the arrow shows the direction of shift in the (a) excitatory synapse with increasing duration of pulses, (b) excitatory synapse with increasing pulse number, (c) inhibitory synapse with increasing duration of the pulse, and (d) inhibitory synapse with the increasing number of pulses.

the STM-to-LTM alteration is achieved in excitatory and inhibitory synapses with increasing duration and count of optical pulses.

Along with the changes in stimuli properties, solvent polarity also enhances the plasticity of the studied synapse. The polarity of the solvent affects the ground state and excited state

energy levels of merocyanine, leading to varied colors of the intermediate state.<sup>53</sup> In non-polar solvents, the isomerization reaction is a non-spontaneous process that requires UV irradiation. The merocyanine in that case appears blue due to shifted energy band positions (details in ESI<sup>†</sup>). This solvatochromic effect is utilized to vary the synaptic plasticity. Equimolar

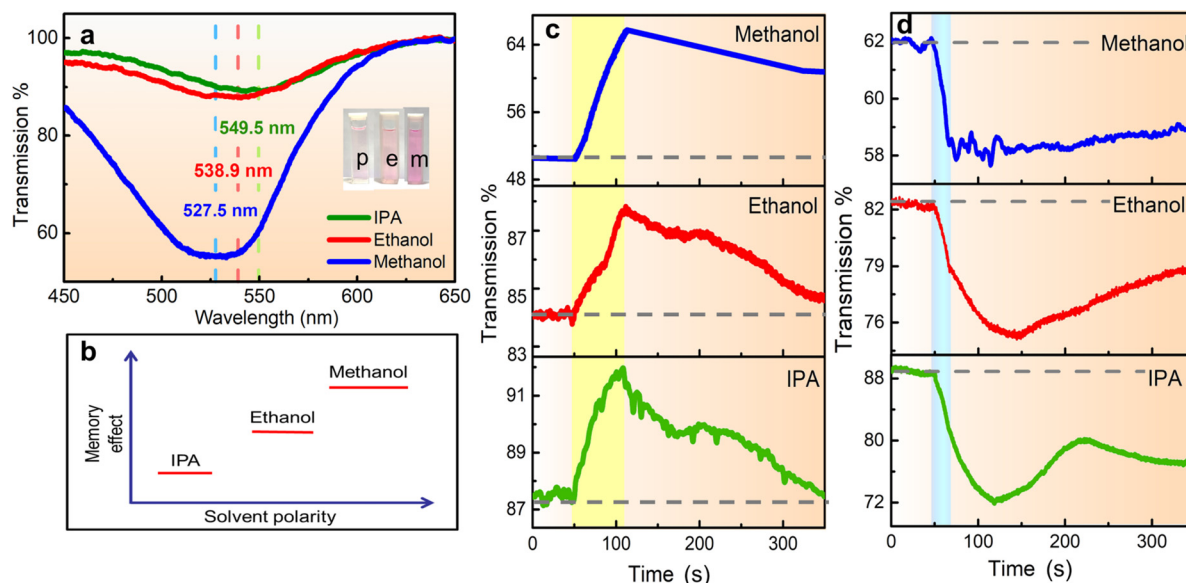


**Fig. 5** (a) Transmission spectra show a blueshift of  $\lambda_{\min}$  and decreased transmission intensity at  $\lambda_{\min}$  with increasing solvent polarity in the dark. (b) An increase in solvent polarity increases the merocyanine isomers and the memory effect. Comparison of plasticity in IPA (p), ethanol (e), and methanol (m) with a single (c) excitatory pulse (visible) and (d) inhibitory pulse (UV). Greater solvent polarity leads to greater plasticity for both excitatory and inhibitory synapses.

solutions of spiropyran in methanol, ethanol, and isopropyl alcohol (IPA) are studied (see Fig. 5(a)).

The solvent polarity increases in the order of isopropyl alcohol (IPA), ethanol, and methanol. With increasing polarity,  $\lambda_{\min}$  and the transmission value at  $\lambda_{\min}$  decreases. The blue-shift in  $\lambda_{\min}$  is due to expanding merocyanine bandgap, while the lower transmission values are because of more converted merocyanine. The intermediate color of the solution in IPA, ethanol, and methanol is shown in the inset of Fig. 5(a), where the pink color is intense in methanol (the solvent with the highest polarity studied here). Since the transmission of the intermediate state is different for every solvent, the relative change of transmittance upon irradiation with visible and UV pulses also varies. The excitatory synaptic activity with 60 s visible pulse and inhibitory synaptic activity with 15 s UV pulse are presented in Fig. 5(c) and (d), respectively. The synaptic plasticity increases in the order of IPA, ethanol, and methanol, consistent with increasing polarity. Since plasticity is directly associated with memory, increasing the solvent polarity improves memory (Fig. 5(b)) in excitatory and inhibitory photonic synapses. Furthermore, to improve the response time of all-optical artificial synapses, the intensity of light and concentration of the solution can be changed. Not only this, changing the nature of the solvent and the substituents in the spiropyran can also affect the response time. The molecular environment changes the activation energy required for C–O bond cleavage, changing the overall rate and other properties.

Also, the power consumption for an all-optical artificial synapse can be determined by calculating the energy of the optical pulse ( $E$ ) per unit area ( $A$ ) for an exposure time ( $t$ ) of 1 s.

$$P = \frac{E}{t \cdot A}$$

So, the power consumptions for the excitatory (visible pulse) and inhibitory (UV pulse) synapses are  $0.1 \text{ mW cm}^{-2}$  and  $0.4 \text{ mW cm}^{-2}$ , respectively. However, this power consumption can be reduced by minimizing the optical pulse energy, device size, and exposure time.

To facilitate the integration of the spiropyran-based photonic synapse with solid-state devices, further experiments are performed by dispersing spiropyran in poly(methyl methacrylate) (PMMA) polymer and spin coating it onto quartz substrates. The results (presented in ESI†) confirm the switching of isomers with light irradiation, highlighting the method's utility for solid-state devices.

In conclusion, we demonstrate an all-optical artificial synapse using a reversible, high-contrast photochromic compound, spiropyran. The photochromic and solvatochromic properties of spiropyran are utilized to mimic biological synaptic activities. The quantal changes in transmittance during spiropyran–merocyanine isomerization cycles with visible and UV pulses are equated to memory and learning. Excitatory and inhibitory synaptic activities are emulated with visible and UV pulses. Short-term memory (STM), long-term memory (LTM), and transition from STM-to-LTM necessary for cognition development is achieved by controlling the duration and the number of stimulating excitations. Solvatochromism is also exploited to

enhance the plasticity of such synapses. This study demonstrates the utility of spiropyran as a suitable candidate for all-optical artificial synapses and elucidates photochromic compounds as excellent hosts for photonic synapses for brain-inspired computing.

## Author contributions

DS and DR performed all experiments and analysed the results. BS conceived and administered the project. All authors discussed and contributed in writing the manuscript.

## Conflicts of interest

There are no conflicts to declare.

## Acknowledgements

DS and BS acknowledge International Centre for Materials Science (ICMS) and Sheikh Saqr Laboratory (SSL) in JNCASR for support. BS acknowledges the Science and Engineering Research Board (SERB) of the Government of India, Start-Up Research Grant no. SRG/2019/000613 for financial support. DS and DR thank JNCASR for the fellowship. DR acknowledges SAMat research facilities. DS and BS acknowledge Anshulata and Prof. Bani Kanta Sarma for assistance with NMR experiments.

## References

- 1 D. S. Jeong and C. S. Hwang, *Adv. Mater.*, 2018, **30**, 1–27.
- 2 X. Zou, S. Xu, X. Chen, L. Yan and Y. Han, *Sci. China Inf. Sci.*, 2021, **64**, 160404.
- 3 H. Li, X. Jiang, W. Ye, H. Zhang, L. Zhou, F. Zhang, D. She, Y. Zhou and S. T. Han, *Nano Energy*, 2019, **65**, 104000.
- 4 S. Jiang, S. Nie, Y. He, R. Liu, C. Chen and Q. Wan, *Mater. Today Nano*, 2019, **8**, 100059.
- 5 H. Moravec, *J. Evol. Technol.*, 1998, **1**, 10.
- 6 J. Zhang, Basic Neural Units of the Brain: Neurons, Synapses and Action Potential, *arXiv*, 2019, preprint, arXiv:1906.01703, DOI: [10.48550/arXiv.1906.01703](https://doi.org/10.48550/arXiv.1906.01703).
- 7 D. J. Bakkum, U. Frey, M. Radivojevic, T. L. Russell, J. Müller, M. Fiscella, H. Takahashi and A. Hierlemann, *Nat. Commun.*, 2013, **4**, 2181.
- 8 X. Zhuge, J. Wang and F. Zhuge, *Phys. Status Solidi RRL*, 2019, **13**, 1–15.
- 9 A. E. Pereda, *Nat. Rev. Neurosci.*, 2014, **15**, 250–263.
- 10 J. Sawada, F. Akopyan, B. L. Jackson, N. Imam, C. Guo, R. Appuswamy, B. Taba, A. Amir, M. D. Flickner, P. A. Merolla, J. V. Arthur, R. Alvarez-icaza, A. S. Cassidy, J. Sawada, F. Akopyan, B. L. Jackson, N. Imam, C. Guo, Y. Nakamura, B. Brezzo, I. Vo, S. K. Esser, R. Appuswamy, B. Taba, A. Amir, M. D. Flickner, W. P. Risk, R. Manohar and D. S. Modha, *Science*, 2014, **345**, 668–673.
- 11 M. Davies, N. Srinivasa, T. H. Lin, G. China, Y. Cao, S. H. Choday, G. Dimou, P. Joshi, N. Imam, S. Jain, Y. Liao,

- C. K. Lin, A. Lines, R. Liu, D. Mathaikutty, S. McCoy, A. Paul, J. Tse, G. Venkataramanan, Y. H. Weng, A. Wild, Y. Yang and H. Wang, *IEEE Micro.*, 2018, **38**, 82–99.
- 12 J. Tang, F. Yuan, X. Shen, Z. Wang, M. Rao, Y. He, Y. Sun, X. Li, W. Zhang, Y. Li, B. Gao, H. Qian, G. Bi, S. Song, J. J. Yang and H. Wu, *Adv. Mater.*, 2019, **31**, 1902761.
- 13 D. B. Strukov, G. S. Snider, D. R. Stewart and R. S. Williams, *Nature*, 2008, **453**, 80–83.
- 14 L. Kortekaas and W. R. Browne, *Chem. Soc. Rev.*, 2019, **48**, 3406–3424.
- 15 S. G. Kim, J. S. Han, H. Kim, S. Y. Kim and H. W. Jang, *Adv. Mater. Technol.*, 2018, **3**, 1800457.
- 16 Y. Chen, H. Yu, J. Gong and M. Ma.
- 17 M. Xu, X. Mai, J. Lin, W. Zhang, Y. Li, Y. He, H. Tong, X. Hou, P. Zhou and X. Miao, *Adv. Funct. Mater.*, 2020, **30**, 1–21.
- 18 I. Chakraborty, G. Saha and K. Roy, *Phys. Rev. Appl.*, 2019, **11**, 1.
- 19 P. B. Pillai and M. M. De Souza, *ACS Appl. Mater. Interfaces*, 2017, **9**, 1609–1618.
- 20 R. Yang, K. Terabe, Y. Yao, T. Tsuruoka, T. Hasegawa, J. K. Gimzewski and M. Aono, *Nanotechnology*, 2013, **24**, 384003.
- 21 J. Hong, X. Li, N. Xu, H. Chen, S. Cabrini, S. Khizroev, J. Bokor and L. You, *Adv. Intell. Syst.*, 2020, **2**, 2000143.
- 22 D. W. Kim, W. S. Yi, J. Y. Choi, K. Ashiba, J. U. Baek, H. S. Jun, J. J. Kim and J. G. Park, *Front. Neurosci.*, 2020, **14**, 1–9.
- 23 D. Xie, K. Yin, Z. J. Yang, H. Huang, X. Li, Z. Shu, H. Duan, J. He and J. Jiang, *Mater. Horiz.*, 2022, **9**, 1448–1459.
- 24 Y. Li, T. Chen, X. Ju and T. Salim, *Nanoscale*, 2022, **14**, 10245–10254.
- 25 L. Shao, Y. Zhao and Y. Liu, *Adv. Funct. Mater.*, 2021, **31**.
- 26 X. Wan, Y. Yang, P. Feng, Y. Shi and Q. Wan, *IEEE Electron Device Lett.*, 2016, **37**, 299–302.
- 27 S. Maren and M. Baudry, *Neurobiol. Learn. Mem.*, 1995, **63**, 1–18.
- 28 D. Rosenbluth, K. Kravtsov, M. P. Fok and P. R. Prucnal, *Opt. Express*, 2009, **17**, 22767.
- 29 M. Qi, X. Zhang, L. Yang, Z. Wang, H. Xu, W. Liu, X. Zhao and Y. Liu, *Appl. Phys. Lett.*, 2018, **113**, 1–6.
- 30 Y. C. Chiang, C. C. Hung, Y. C. Lin, Y. C. Chiu, T. Isono, T. Satoh and W. C. Chen, *Adv. Mater.*, 2020, **32**, 1–8.
- 31 Z. Xiao and J. Huang, *Adv. Electron. Mater.*, 2016, **2**, 1600100.
- 32 W. Cao, J. Jiang, X. Xie, A. Pal, J. H. Chu, J. Kang and K. Banerjee, *IEEE Trans. Electron Devices*, 2018, **65**, 4109–4121.
- 33 Z. C. Zhang, Y. Li, J. J. Wang, D. H. Qi, B. W. Yao, M. X. Yu, X. D. Chen and T. B. Lu, *Nano Res.*, 2021, **14**, 4591–4600.
- 34 Y. Shi, X. Liang, B. Yuan, V. Chen, H. Li, F. Hui, Z. Yu, F. Yuan, E. Pop, H. S. P. Wong and M. Lanza, *Nat. Electron.*, 2018, **1**, 458–465.
- 35 T. Y. Wang, J. L. Meng, Z. Y. He, L. Chen, H. Zhu, Q. Q. Sun, S. J. Ding, P. Zhou and D. W. Zhang, *Adv. Sci.*, 2020, **7**, 1903480.
- 36 A. J. Arnold, A. Razavieh, J. R. Nasr, D. S. Schulman, C. M. Eichfeld and S. Das, *ACS Nano*, 2017, **11**, 3110–3118.
- 37 S. Seo, S. H. Jo, S. Kim, J. Shim, S. Oh, J. H. Kim, K. Heo, J. W. Choi, C. Choi, S. Oh, D. Kuzum, H. S. P. Wong and J. H. Park, *Nat. Commun.*, 2018, **9**, 1–8.
- 38 G. di Martino and S. Tappertzhofen, *Nanophotonics*, 2019, **8**, 1579–1589.
- 39 Y. Wang, L. Yin, W. Huang, Y. Li, S. Huang, Y. Zhu, D. Yang and X. Pi, *Adv. Intell. Syst.*, 2021, **3**, 2000099.
- 40 J. Zhang, S. Dai, Y. Zhao, J. Zhang and J. Huang, *Adv. Intell. Syst.*, 2020, **2**, 1900136.
- 41 C. Li, W. Du, Y. Huang, J. Zou, L. Luo, S. Sun, A. O. Govorov, J. Wu, H. Xu and Z. Wang, *Opto-Electron. Adv.*, 2020, 210069.
- 42 B. Gholipour, P. Bastock, C. Craig, K. Khan, D. Hewak and C. Soci, *Adv. Opt. Mater.*, 2015, **3**, 635–641.
- 43 Z. Cheng, C. Ríos, W. H. P. Pernice, C. David Wright and H. Bhaskaran, *Sci. Adv.*, 2017, **3**, 1–7.
- 44 H. Markram, W. Gerstner and P. J. Sjöström, *Front. Synaptic Neurosci.*, 2012, **4**, 2010–2012.
- 45 J. Zhang, Q. Zou and H. Tian, *Adv. Mater.*, 2013, **25**, 378–399.
- 46 R. Klajn, *Chem. Soc. Rev.*, 2014, **43**, 148–184.
- 47 H. Görner, *Phys. Chem. Chem. Phys.*, 2001, **3**, 416–423.
- 48 B. R. Heiligman-rim and Y. Hieshbeeg, *J. Chem. Soc.*, 1961, 156–163.
- 49 W. Tian and J. Tian, *Dyes Pigm.*, 2014, **105**, 66–74.
- 50 M. Karcher, C. Rüdte, C. Elsässer and P. Fumagalli, *J. Appl. Phys.*, 2007, **102**, 1–6.
- 51 S. J. Martin, P. D. Grimwood and R. G. Morris, *Annu. Rev. Neurosci.*, 2000, **23**, 649–711.
- 52 S. Gao, G. Liu, H. Yang, C. Hu, Q. Chen, G. Gong, W. Xue, X. Yi, J. Shang and R. W. Li, *ACS Nano*, 2019, **13**(2), 2634–2642.
- 53 M. Taguchi, G. Li, Z. Gu, O. Sato and Y. Einaga, *Chem. Mater.*, 2003, **15**, 4756–4760.